**International Journal of Power Electronics and Drive System (IJPEDS)**
Vol. 17, No. 1, March 2026, pp. 107~122
ISSN: 2088-8694, DOI: 10.11591/ijpeds.v17.i1.pp107-122 

# Fuzzy adaptive sliding mode control with exponential reaching law for enhanced 4WD electric vehicle speed control

**Abdelhamid Bouregba[1], Abdeldjabar Hazzab[2], Aissa Benhammou[1], Samir Hadjeri[3]**
[1]Department of Electrotechnical, Faculty of Electrical Engineering, Djillali Liabes University, Sidi Bel Abbès, Algeria
[2]Department of Electrical Engineering, École de Technologie Supérieure, Montréal, Canada
[3]Department of Electrical Engineering, Faculty of Technology, Mohamed Tahri University, Bechar, Algeria

**Article Info**

***Article history:***

Received Sep 23, 2025
Revised Jan 11, 2026
Accepted Jan 23, 2026

***Keywords:***

4 wheel-drive
Classical SMC
Electric vehicle
Exponential reaching law
Induction motor

**ABSTRACT**

This paper discusses a novel fuzzy adaptive sliding mode control (FASMC) strategy for a four-wheel-drive (4WD) electric vehicle (EV), incorporating an exponential reaching law (ERL) and a fuzzy adaptive switching gain to enhance speed tracking. The classical SMC technique often suffers from the chattering problem, which can degrade the dynamic control performance of the electric vehicle. To address these challenges, the proposed hybrid controller employs an exponential reaching law to ensure fast convergence and reduced chattering, while a fuzzy logic-adaptation mechanism dynamically adjusts the switching gain to improve robustness against uncertainties and external disturbances. First, the mathematical model of the motor derived for achieving speed regulation using the classical SMC with an exponential reaching law based on indirect-field-oriented control (FOC). Then, the proposed control technique is designed to automatically adjust the ERL gain using a fuzzy logic controller to ensure precise vehicle speed control, optimizing the vehicle's dynamics under varying road conditions. This novel configuration enables the development of a 4WD EV control framework with an optimized controller, serving as the foundation for implementing our proposed study. The results validate the proposed method's superiority, delivering lower chattering, enhanced tracking precision, and greater robustness compared to traditional SMC while adhering to control standards. This control framework presents a viable advancement for 4WD EV motion management, supporting safer, more effective autonomous vehicle technologies.



***Corresponding Author:***

Abdelhamid Bouregba
Department of Electrotechnical, Faculty of Electrical Engineering, Djillali Liabes University
Sidi Bel Abbès, Algeria
Email: hamidgourarii@gmail.com

## 1. INTRODUCTION

Recently, the automotive industry has known a significant interest in the adoption of electric drives for vehicle traction, for reasons of sustainability, emissions reductions, and energy efficiency [1]. This transition has led to the widespread development of various types of EVs, including EV's battery, hybrid EV modes, and fuel cell-powered EVs. As a result, drivetrain technologies have become a focal point of research and innovation, with a strong emphasis on improving efficiency, performance, and reliability for the foreseeable future. A vehicle's driving performance is typically assessed based on key metrics such as acceleration time, maximum velocity, and road gradeability. At the heart of the electric propulsion system lies the electrical motor, which serves as its essential component. Recently, leading international vehicle

manufacturers have increasingly employed induction motors (IMs) and permanent magnet motors (PMs) in their electric vehicle designs due to their high efficiency, reliability, and adaptability [2].

According to industry evaluations and surveys conducted among electric vehicle commercial companies, the IM has emerged as a preferred choice for electric vehicle drivetrain systems (EVDS) due to its robustness, lower cost, and ability to operate effectively under a wide range of conditions [3]. Control of speed in electric vehicles (EVs) is crucial for enhancing the performance, efficiency, and general functionality of EV traction systems. As an important part of the electric powertrain, speed regulation lets the car adapt to different driving conditions, such as sudden acceleration, deceleration, or changes in road gradient, while still keeping smooth and precise control over how the motor operates [4].

In fact, the IM presents a high coupling between flux and torque. making the control of induction motors more challenging, as adjustments to one parameter inevitably influence the other. To address this complexity, the researchers have developed many control propositions, such as scalar control, vector control, or field-oriented control (FOC). The scalar control technique is widely recognized for its simple structure and ease of implementation, making it an attractive solution that can provide acceptable steady-state performances for IM drive control. Yet scalar control reveals limitations under transients, including abrupt load or speed variations. Vector control allows for accurate and smooth control of both flux and torque, even during rapid changes in operating conditions. However, this technique has a high sensitivity to the machine parameters variations and requires a precise mathematical model of the IM, accurate measurement, and sophisticated control method, increasing the complexity in terms of hardware requirements, computational resources, and implementation [5].

The proposition of an adaptive neural fuzzy inference system (ANFIS) by Benhammou *et al.* [2], it has resulted in some ripples in the law speed test due to the requirement adaptation of the controllers. However, the discontinuous nature of the control law in SMC can lead to high-frequency switching, also known as the chattering phenomenon, which can propagate throughout the system and cause a range of undesirable effects [6]. To mitigate these limitations, various methods and advanced propositions have been developed to minimize chattering while preserving SMC robustness and dynamic performances [7]. One such method is the boundary-layer strategy, which introduces a smooth transition region around the sliding surface. This approach maintains the system's stability and robustness while significantly improving control smoothness [8]. However, it has several limitations, including reduced robustness, residual chattering, and challenges in tuning the boundary layer thickness. To address these issues, several advanced and hybrid control strategies are often employed, such as higher-order sliding mode control and methods that combine SMC with adaptive control and intelligence techniques, such as neural networks and fuzzy logic.

The goal of the paper is to investigate an adaptive sliding mode control (ASMC) based on exponential reaching law design using a fuzzy logic system for 4WDEV speed control. The outer speed loop employs a fuzzy adaptive sliding mode control (FASMC) to achieve superior performance, minimize chattering, guarantee stability/robustness, and improve EV dynamic response [4]. Analysis of recent research in [9], a hybrid fuzzy sliding mode control (SMC) regulates doubly fed induction generator (DFIG) active/reactive power in wind energy conversion systems (WECS), minimizing chattering while delivering robust, precise performance amid disturbances. In [10], a robust sliding mode control scheme is proposed, incorporating an adaptive switching gain and an integral action to effectively mitigate the influence of model uncertainties and external disturbances.

In [11], a fast and smooth second-order sliding mode control approach is introduced to enhance power extraction performance in fixed-pitch, variable-speed WECS. Moreover, a neuro-fuzzy scheme founded on the Takagi-Sugeno-Kang (TSK) inference structure is employed to improve robustness and to provide reliable online estimation of system parameters under uncertain operating conditions [12]. Furthermore, Nurettin and Inanç have presented a hybrid fuzzy super-twisting sliding mode controller (HFSTSMC) for IM vector control systems, combining super-twisting sliding mode control (STSMC) with a fuzzy logic controller (FLC) to optimize control coefficients and reduce chattering while maintaining high tracking accuracy and robustness. The authors in [13] introduce a robust trajectory tracking control law for autonomous vehicles using a higher-order quasi-sliding mode control (QSMC) combined with an adaptive single-input FLC, which estimates perturbations online and ensures global asymptotic stability via Lyapunov theory. Another approach proposes a fuzzy adaptive SMC control algorithm to enhance the lateral stability of distributed drive EVs by addressing system parameter perturbations and external disturbances, using a simplified unscented Kalman filter observer to estimate critical vehicle state parameters and road adhesion coefficients [14]. Optimized fuzzy control for quadcopters to enhance their behavior has been proposed in [15], where other hybrid control strategies based on adaptive fuzzy sliding mode control have been explored for attitude stabilization of quadrotor unmanned aerial vehicles (UAVs) [16]. In this approach, a fuzzy logic system is employed to approximate system uncertainties, while a second-order auxiliary system is introduced to counteract control input saturation. System stability is ensured through Lyapunov-based analysis. Similarly, an SMC technique for acceleration slip regulation in battery electric vehicles is proposed in [17]. This method effectively addresses wheel slip during initial acceleration by adaptively tuning the switching function of the sliding mode

controller using a fuzzy algorithm. In [18], a novel fuzzy sliding mode proportional-integral control (FSMPIF) strategy is introduced for active suspension systems. By integrating PI control, sliding mode control, and fuzzy logic, this hybrid controller aims to minimize vehicle vibrations and enhance ride comfort. Several advanced control strategies have been explored for electric systems and motion control, including (STSMC) [12], ANFIS [2], model predictive control (MPC) [19], fractional order proportional–integral–derivative (PID) [20], [21], and fuzzy-PI controllers [15]. Each approach offers distinct trade-offs in complexity, adaptability, and required training effort. Compared to these, the proposed FASMC combines rapid convergence and robustness with adaptive tuning, aiming to overcome limitations such as chattering in classical SMC and extensive training in neuro-fuzzy methods. This comparative perspective guides the development of a more efficient and practical control solution. Table 1 compares some controller techniques.

Building on the benefits reported in the aforementioned studies, this work employs a fuzzy logic–based controller to appropriately tune the system parameters, ε and K, in the ERL of the traditional SMC based on an appropriate algorithm to improve the dynamic performances against operating conditions variations and external load. The work presents the proposition of a novel SMC strategy for a 4WD-EV, integrating an ERL and a fuzzy adaptive switching gain to enhance speed tracking performance. It highlights the challenges posed by chattering in classical SMC and how the proposed hybrid controller effectively reduces this issue while improving robustness against uncertainties and disturbances. In general, the main objectives of this study can be summarized as follows:

- A mathematical design procedure of a speed controller based on indirect FOC 4WDEV.
- The sliding mode control challenges are reduced first using an exponential reaching law.
- The parameters of the exponential reaching law are automatically changed by a fuzzy logic system designed based on the transient and steady-state conditions of control system states.

The remainder of this paper is structured as follows: i) Section 2 describes the comprehensive modeling of the EV propulsion system; ii) The formulation of the sliding mode speed controller for the induction motor, incorporating an exponential reaching law, is detailed in Section 3; iii) Section 4 presents the development of the FASMC scheme; iv) The electronic differential mechanism implemented for vehicle operation is discussed in Section 5; and v) Section 6 reports and analyzes the simulation results that demonstrate the effectiveness of the proposed control strategies. Concluding remarks and perspectives for future research are given in the final section.

Table 1. Different control techniques comparison

| Criterion | STSMC [12] | ANFIS [2] | MPC [19] | Fuzzy-PID [15] |
|---|---|---|---|---|
| Complexity | Medium; requires gain tuning and chattering | Requires data training and network tuning | Needs precise modelling and real computation | Low to medium; simpler tuning |
| Adaptability | Good; robust to disturbances | Good | Very good; anticipates and optimizes control | Moderate; limited by fuzzy rules design |
| Training effort | Low; basic tuning needed | High; requires substantial training data | Medium to high; | Low; requires initial fuzzy rule setup |
| Control performance | Good stability; chattering possible | Superior responsiveness; adaptive to changes | Excellent constraint handling and prediction | Moderate performance |

## 2. MODELLING OF EV DRIVING

Effective speed control in accordance with a predefined driving cycle requires a comprehensive vehicle model. The vehicle model receives the reference velocity from the predefined driving cycle as its input, while the control system interfaces directly with the inverter. The inverter plays a crucial role by converting the DC electrical energy from the battery into controlled AC voltage and current supplied to the induction motor. The IM then converts this electrical energy into mechanical power, which ultimately propels the vehicle. Figure 1 illustrates the main components of the electric vehicle propulsion system and emphasizes their coordinated integration to ensure efficient and responsive vehicle operation [22].

### 2.1. EV dynamic model

The use of a dynamic vehicle model is essential for improving the overall efficiency of EVs, as it enables the optimization of propulsion system design and the assessment of vehicle performance under realistic operating conditions. Consider an EV of mass $M_v$ traveling at a velocity V on a roadway inclined at an angle $\delta$ relative to the horizontal. The vehicle dynamics can be described by modeling the EV as a rigid body subjected to several longitudinal resistive forces. These forces include aerodynamic drag arising from air–vehicle interaction, rolling resistance due to tire–road contact, grade resistance induced by road slope, and inertial resistance associated with variations in vehicle speed. The combined effect of these forces determines the total traction force required for vehicle motion and directly influences energy consumption as well as the effectiveness of the applied control strategies, as depicted in Figure 2 [8].

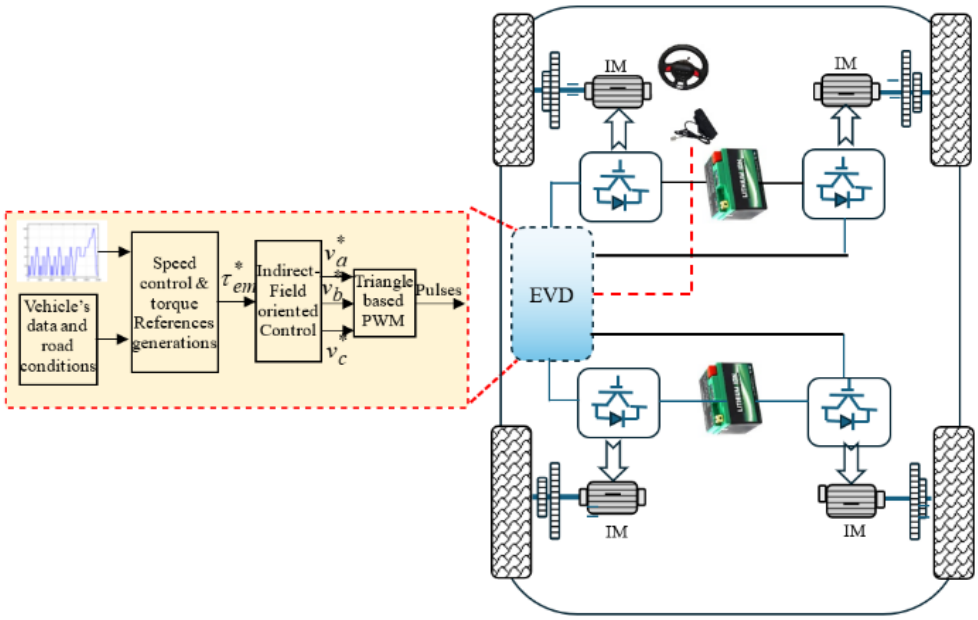


Figure 1. The constituent elements of the EV propulsion system

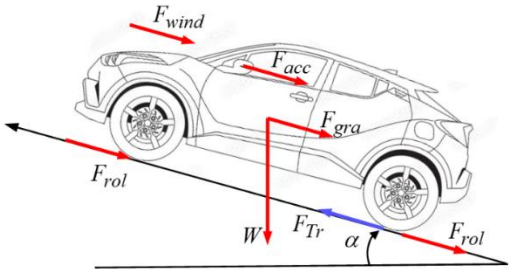


Figure 2. Illustrates the forces acting on the 4WD

Based on these forces, the vehicle dynamics can be described using Newton's second law as (1).

$$M_v \frac{d\vec{v}}{dt} = \sum \vec{F}_{ext} = \vec{F}_{Tr} + \vec{F}_{acc} + \vec{F}_{rol} + \vec{F}_{wind} + \vec{F}_{gra} \quad (1)$$

The projection of the law onto the horizontal axis leads to (2):

$$M_v \frac{dv}{dt} = \sum F_{ext} = F_{Tr_x} - \left(F_{acc_x} + F_{rol_x} + F_{wind_x} + F_{gra_x}\right) \quad (2)$$

where:

$$F_{wind_x} = \frac{1}{2}\rho S C_x (v - v_0)^2 \quad (3)$$

$$F_{gra_x} = G_r M_v g \cos(\alpha) \quad (4)$$

$$W_x = M_v g \sin(\alpha) \quad (5)$$

$$F_{acc_x} = M_v \frac{dv}{dt} \quad (6)$$

Where $F_{Tr}$ represents the total tractive force, $F_{wind}$ the force of wind resistance, $F_{rol}$ the force of rolling resistance, $F_{gra}$ the force of grading resistance, $F_{acc}$ the force of acceleration, and $C_{win}$, and $C_{rol}$ symbolize the wind and rolling resistance coefficient, respectively, while $m$ is the vehicle mass, and $g$ is the gravitational force. The wheel radius, gear ratio, and vehicle velocity are represented by $w_r$, $G_r$, and $V_V$, respectively.

$$\omega_r = G_r \frac{V_v}{R_{wheel}}, \text{ and } \omega_{wheel} = \frac{V_v}{R_{wheel}} \quad (7)$$

The motor load torque $T_L$ can be formulated as a function of speed as (8).

$$T_L = \frac{1}{G_r} T_w = \frac{1}{G_r}\left(F_{wind} + F_{rol} + F_{acc} + F_{gra}\right) \quad (8)$$

### 2.2. The system modeling

The dynamic behavior of the three-phase Y-connected induction motor can be expressed in the synchronous d-q reference frame through the following set of differentials in (9)-(13) [23], [24]:

$$\frac{di_{ds}}{dt} = \frac{1}{\sigma L_s}\left(-R_{eq} i_{ds} + \sigma L_s \omega_s i_{qs} + \frac{L_m R_r}{L_r^2}\varphi_{dr} + P\frac{L_m}{L_r}\varphi_{qr}\omega_r + v_{ds}\right) \quad (9)$$

$$\frac{\mathrm{di_{qs}}}{\mathrm{dt}} = \frac{1}{\sigma \mathrm{L_s}}\left(-\sigma \mathrm{L_s}\omega_s \mathrm{i_{ds}} - \mathrm{R_{eq}} \mathrm{i_{qs}} - \mathrm{P}\frac{\mathrm{L_m}}{\mathrm{L_r}}\varphi_{\mathrm{dr}}\omega_{\mathrm{r}} + \frac{\mathrm{L_m R_r}}{\mathrm{L_r^2}}\varphi_{\mathrm{qr}} + \mathrm{v_{qs}}\right) \quad (10)$$

$$\frac{d\varphi_{dr}}{dt} = \frac{L_m R_r}{L_r} i_{ds} - \frac{R_r}{L_r}\varphi_{dr} + (\omega_s - P\omega_r)\varphi_{qr} \quad (11)$$

$$\frac{d\varphi_{qr}}{dt} = \frac{L_m R_r}{L_r}. i_{qs} - (\omega_s - P\omega_r). \varphi_{dr} - \frac{R_r}{L_r}. \varphi_{qr} \quad (12)$$

$$\frac{d\omega_r}{dt} = \frac{1}{J}\left(\frac{3}{2}\frac{P.L_m}{L_r}.\left(i_{qs}.\varphi_{dr} - i_{ds}.\varphi_{qr}\right) - f_c.\omega_r - .T_l\right) \quad (13)$$

where $R_s$, $R_r$ denote the stator and rotor resistors, $L_m$ is the magnetizing inductance per phase. $L_s$ , $L_r$ are the stator inductance and rotor inductance per phase, $\omega_s$ denotes the synchronous frequency and $\omega_r$ is the rotor frequency, $P$ the number of pole pairs, $\tau_r = L_r/R_r$ the rotor time-constant, $\sigma = 1 - [L_m^2/(L_s L_r)]$ represents the leakage coefficient, $i_{ds}$ and $i_{qs}$ d-axis and q-axis stator current, $\varphi_{dr}$ and $\varphi_{qr}$ d-axis and q-axis rotor flux, $v_{ds}$ and $v_{qs}$ are the d-axis and q-axis stator voltage, $R_{eq} = (R_s + (L_m/L_r)^2 R_r)$. And the electromagnetic torque can be written as given in (14).

$$T_e = \frac{3PL_m}{2L_r}\left(i_{qs}\varphi_{dr} - i_{ds}\varphi_{qr}\right) \quad (14)$$

Under vector control, the induction motor exhibits dynamic characteristics analogous to those of a separately excited DC machine, allowing independent regulation of torque and flux. When perfect rotor flux orientation is achieved, the quadrature component of the rotor flux$\varphi_{qr}$, becomes zero. Consequently, the system equations can be expressed as shown in (15) and (16):

$$\varphi_{qr} = 0 \quad (15)$$

$$\varphi_{dr} = \varphi_r^N = \text{constant} \quad (16)$$

where: $\varphi_r^N$ is the rotor flux rated value. Consequently, the torque equation is simplified to become like a DC motor torque equation as (17).

$$T_e = \frac{3PL_m}{2L_r} i_{qs}\varphi_{dr} \quad (17)$$

And the slip frequency, $\omega_{sl} = \omega_s - P\omega_r$, is computed by (18):

$$\omega_{sl} = \frac{1}{\tau_r}\frac{i_{qs}^*}{i_{ds}^*} \quad (18)$$

where superscript (*) represents reference values.

## 3. SLIDING MODE CONTROL BASED ON EXPONENTIAL REACHING LAW FOR IM SPEED CONTROL

SMC is a form of variable structure control. It is recognized as an excellent technique for robust controller design applicable to diverse complex nonlinear systems functioning under various unpredictable

conditions [14], [25]. The SMC offers numerous undeniable benefits, including resilience to external disturbances, accuracy, stability, and insensitivity to parameter variations within the controlled system. As a result, SMC has become a widely adopted approach in multiple scientific and engineering fields, such as electric drives, robotics, nonlinear process regulation, and automotive systems. The primary objective of SMC is to guide the system trajectories toward a designated sliding surface and maintain their motion along it through an appropriate switching control strategy [25]-[27].

When the tracking error is considered as the sliding surface (or switching function) in the speed control loop, it can be represented as (19):

$$s_\omega = e_\omega = \omega_r^* - \omega_r \tag{19}$$

where $\omega_r^*$ represents the desired speed. The derivative of the surface is found as (20).

$$\begin{aligned} \dot{s}_\omega &= \dot{\omega}_r^* - \omega_r^{'} \\ &= \dot{\omega}_r^* - \left(\frac{3}{2}\frac{pL_m}{JL_r}\varphi_{dr} i_{qs} - \frac{f_c}{J}\omega_r - \frac{T_l}{J}\right) \end{aligned} \tag{20}$$

The exponential reaching law is employed to enhance the dynamic performance of the system during the approach phase. It can be mathematically expressed as (21):

$$\dot{s}_\omega = -\varepsilon\, sgn(s_\omega) - k \cdot s_\omega \tag{21}$$

where e and k are positive constants. According to the principle of equivalent control, we can get (22).

$$\begin{cases} \dot{s}_\omega = \dot{\omega}_r^* - \left(\frac{3}{2}\frac{pL_m}{JL_r}\varphi_{dr} i_{qs} - \frac{f_c}{J}\omega_r - \frac{T_l}{J}\right) \\ \quad = -\varepsilon\, sgn(s_\omega) - k \cdot s_\omega \end{cases} \tag{22}$$

The q-axis current $i_{qs}$ expression can be obtained as (23).

$$i_{qs} = \frac{2}{3}\frac{JL_r}{pL_m\varphi_{dr}}\begin{pmatrix} \dot{\omega}_r^* + \frac{f_c}{J}\omega_r + \frac{T_l}{J} + \varepsilon\, sgn(s_\omega) \\ +k \cdot s_\omega \end{pmatrix} \tag{23}$$

The Lyapunov function selected for the sliding mode control system is defined as (24).

$$V = \frac{1}{2}s_\omega^2 \tag{24}$$

The derivative of (14) gives (25).

$$\dot{V} = \dot{s}_\omega s_\omega \tag{25}$$

Then we can get (26).

$$\begin{cases} \dot{V} = s_\omega(-\varepsilon\, sgn(s_\omega) - k \cdot s_\omega) \\ \quad = -\varepsilon\, sgn(s_\omega)\, s_\omega - k \cdot s_\omega^2 \\ \quad = -\varepsilon|s_\omega| - k \cdot s_\omega^2 \le 0 \end{cases} \tag{26}$$

For ensuring high convergence speed, the term $\dot{s}_\omega = -\varepsilon\, sgn(s_\omega)$ is used, while to reduce chattering, we should design a bigger value of $k$ and use a smaller value of $\varepsilon$. for improving the performance of sliding mode control, the smooth function, such as saturation ($\mathrm{sat}(\cdot)$) is used instead of the sign function. The saturation function can be expressed as (27).

$$\mathrm{sat}\left(\frac{s(x)}{\xi}\right) = \begin{cases} \frac{s(x)}{\xi}\, si \left|\frac{s(x)}{\xi}\right| < 1 \\ sgn\left(\frac{s(x)}{\xi}\right) si \left|\frac{s(x)}{\xi}\right| \ge 1 \end{cases} \tag{27}$$

Figure 3 depicts the overall control block diagram of the induction motor speed regulation using SMC with the ERL.

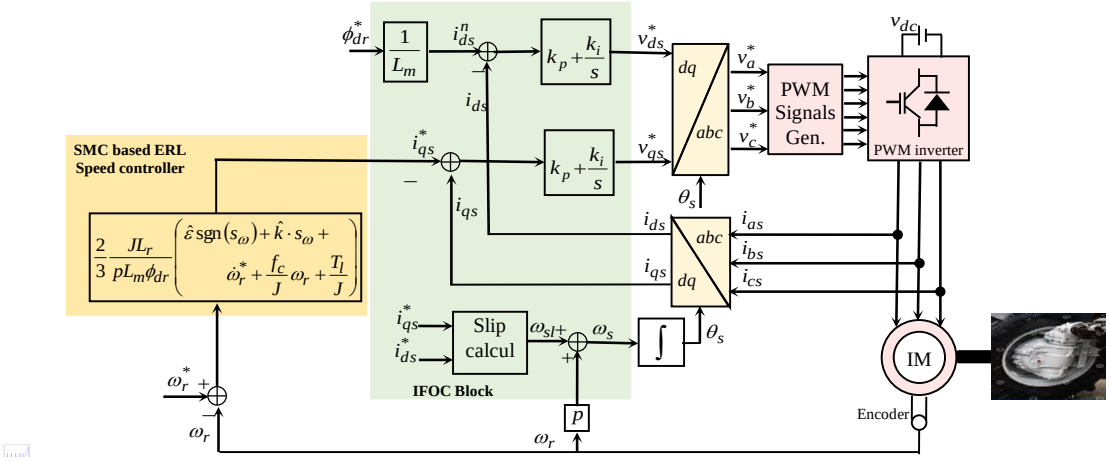


Figure 3. Speed and current control technique based on classical SMC

## 4. PROPOSED ADAPTIVE FUZZY SLIDING MODE CONTROL

In the exponential reaching law, the gains $\varepsilon$ and $k$ remain constant, which can limit the system's dynamic performance and robustness under challenging operating conditions. To overcome this limitation, an FASMC is employed. This controller combines a classical sliding mode controller with a fuzzy logic system that adjusts the parameters based on the transient or steady-state behavior of the system [28], [29]. The operating principle of the proposed adaptive sliding mode control with fuzzy logic adaptation is illustrated in Figure 4. Accordingly, the exponential reaching law of the classical SMC speed control can be expressed as (28) [14].

$$\dot{s}_\omega = -\hat{\varepsilon}\, sgn(s_\omega) - \hat{k} \cdot s_\omega \tag{28}$$

The fuzzy logic controller has two inputs and two outputs. The inputs to the FLC are the sliding surface $s_\omega$ and its derivative$\dot{s}_\omega$ , while the outputs are the switching control parameters ε and k.

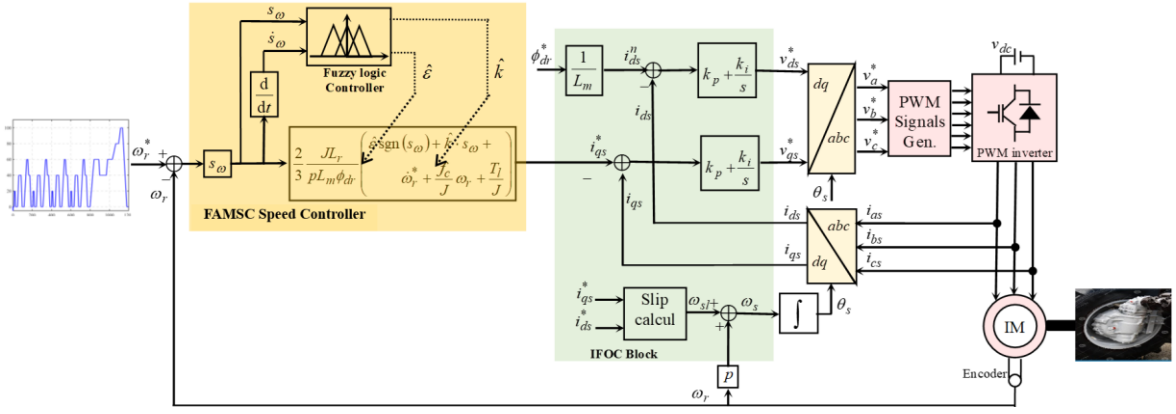


Figure 4. Principle of control system with adaptive fuzzy-SMC

The inference rules are derived from fuzzy sets corresponding to the input variables, which determine the degree of membership of the output variables within their respective subsets. Triangular membership functions are used for the input variables, each of which is defined by five fuzzy sets: big negative (BN), medium negative (MN), zero (Z), medium positive (MP), and big positive (BP). For the outputs of the fuzzy logic adaptation system (FLAS), only three fuzzy subsets are used: S(Small), M (Medium), and B (Big), represented by sigmoid-shaped membership functions. The FASMC utilizes a fuzzy rule base structured as a set of IF-THEN rules that relate the sliding surface and its derivatives to appropriate control actions. The rule base is initially designed based on expert knowledge of the system dynamics and control objectives. Its tuning is achieved through an adaptive mechanism that updates the fuzzy parameters in

real-time, guided by an adaptation law ensuring system stability. This dynamic tuning enables the controller to effectively estimate and compensate for uncertainties and disturbances, improving robustness and tracking performance while minimizing chattering.

The membership functions of the tow inputs,$s_\omega$and $\dot{s}_\omega$, are depicted in Figure 5, whereas the output membership functions of the gain $k_\omega^{fuz}$and the boundary-layer thickness $\xi_\omega^{fuz}$are depicted in Figures 6 and 7, respectively. The membership functions for the two inputs, $s_\omega$ and $\dot{s}_\omega$, are shown in Figure 5, while the output membership functions for the gain $k_\omega^{fuz}$ and the boundary-layer thickness $\xi_\omega^{fuz}$ are illustrated in Figures 6 and 7, respectively.

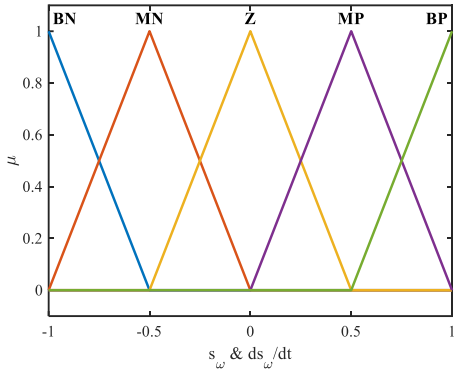


Figure 5. Membership function of the inputs $s_\omega$ and $\dot{s}_\omega$

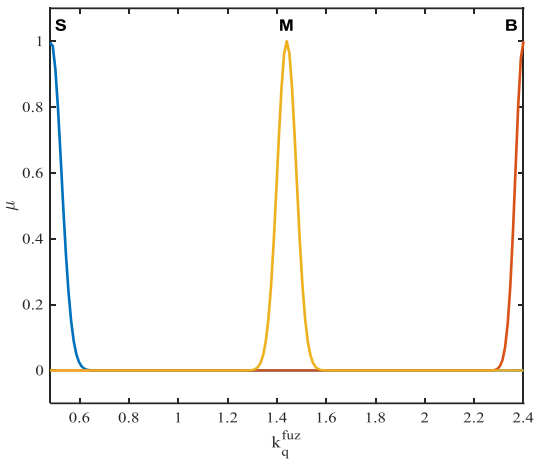


Figure 6. Membership function of the output $k_\omega^{fuz}$

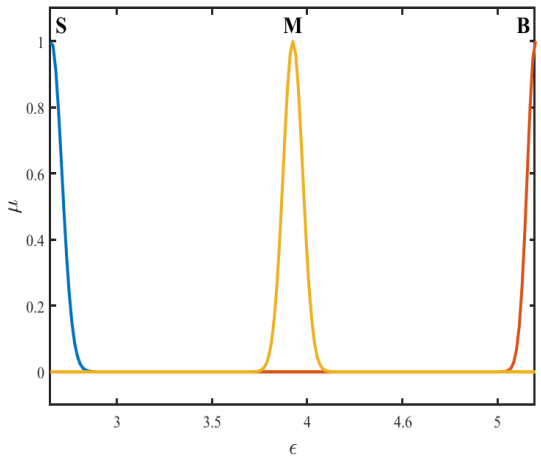


Figure 7. Membership function of the output $\xi_\omega^{fuz}$

Hence, a two-dimensional inference matrix is constructed to organize the rule base governing the adaptive law for both control parameters, ε and *k*, as shown in Tables 2 and 3. Taking the outputs $\hat{\varepsilon}$ and $\hat{k}$ of the fuzzy controller is used as the parameters of the SMC, the expression of the q-axis current is (29).

$$i_{qs} = \frac{2}{3}\frac{JL_r}{pL_m\varphi_{dr}}\left(\dot{\omega}_r^* + \frac{f_c}{J}\omega_r + \frac{T_l}{J} + \hat{\varepsilon}\, sgn(s_\omega) + \hat{k}\cdot s_\omega\right) \tag{29}$$

Based on the stability theorem of SMC, it can be observed that (30) [30].

$$\dot{V} = \dot{s}_\omega s_\omega \tag{30}$$

Then we can get (31).

$$\begin{cases} \dot{V} = s_\omega\left(-\hat{\varepsilon}\, sgn(s_\omega) - \hat{k}\cdot s_\omega\right) \\ \quad = -\hat{\varepsilon}\, sgn(s_\omega)\, s_\omega - \hat{k}\cdot s_\omega^2 \\ \quad = -\hat{\varepsilon}|s_\omega| - \hat{k}\cdot s_\omega^2 \le 0 \end{cases} \tag{31}$$

Therefore, the system is asymptotically stable.

Table 2. FLC rules

| $\hat{k}$ | | $s_\omega$ | | | | |
|---|---|---|---|---|---|---|
| | | BN | MN | Z | MP | BP |
| $\dot{s}_\omega$ | BN | B | B | B | M | S |
| | MN | B | M | M | S | S |
| | Z | M | M | S | M | M |
| | MP | M | S | M | M | B |
| | BP | S | S | B | B | B |

Table 3. Fuzzy rules of the fuzzy adaptation system

| $\hat{\varepsilon}$ | | $s_\omega$ | | | | |
|---|---|---|---|---|---|---|
| | | BN | MN | Z | MP | BP |
| $\dot{s}_\omega$ | BN | S | S | S | M | B |
| | MN | S | M | M | B | B |
| | Z | M | M | B | M | M |
| | MP | M | B | M | M | S |
| | BP | B | B | S | S | S |

## 5. THE ELECTRONIC DIFFERENTIAL PRINCIPLE

The electronic differential system (EDS) for an electric vehicle equipped with four independently driven wheel motors represents a highly complex control architecture. Figure 8 presents the proposed configuration of the electronic differential, in which the front-left and front-right wheels, as well as the rear-left and rear-right wheels, are each controlled by individual motors. IMs are chosen due to their high efficiency, high torque density, quiet operation, and overall suitability for electric vehicle applications [31].

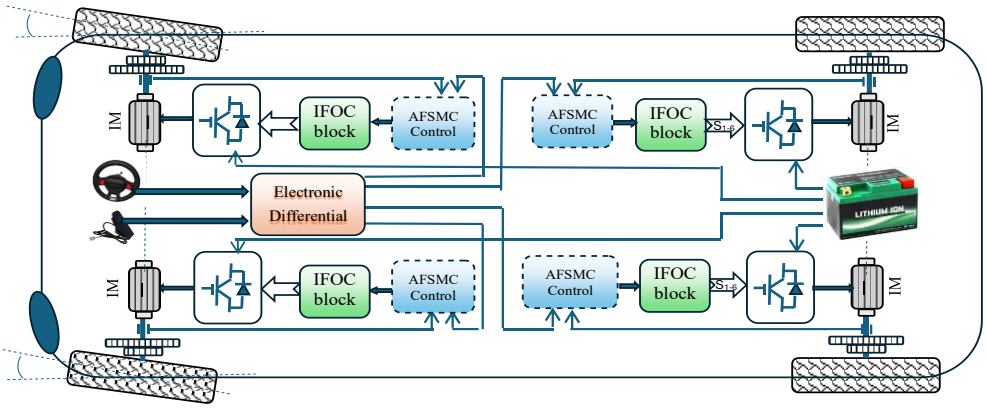


Figure 8. General structure of the EV4WD four-wheel drive electric vehicle studied

The reference speed for the four drive wheels is defined as (32)-(35):

$$\omega_{lr}^* = \omega_{veh}\frac{\sqrt{1+\left(cos(\delta)-\frac{d_\omega}{2L_\omega}\right)^2}}{\sqrt{1+(cos(\delta))^2}} \tag{32}$$

$$\omega_{rr}^* = \omega_{veh}\frac{\sqrt{1+\left(cos(\delta)+\frac{d_\omega}{2L_\omega}\right)^2}}{\sqrt{1+(cos(\delta))^2}} \tag{33}$$

$$\omega_{lf}^* = \omega_{veh}\left(1-\frac{d_\omega\, tan(\delta)}{2L_\omega}\right) \tag{34}$$

$$\omega_{rf}^* = \omega_{veh}\left(1+\frac{d_\omega\, tan(\delta)}{2L_\omega}\right) \tag{35}$$

where: (*) indicates the reference values, $\omega_{lr}$ is the left rear wheel speed, $\omega_{rr}$ is the right rear wheel speed, $\omega_{lf}$ is the left front wheel speed, $\omega_{rf}$, is the right front wheel speed, $\omega_{veh}$ is the EV speed $d_\omega$ and $L_\omega$ are distance between left and right drive wheels and the distance between the front and rear axles.

## 6. SIMULATION RESULTS

To thoroughly assess the performance of the proposed FASMC, a series of simulations encompassing four distinct test scenarios was carried out using the MATLAB/Simulink platform. These test cases were designed to evaluate the controller's effectiveness under various dynamic conditions. The vehicle parameters and system specifications employed in the simulations are detailed in Table 4.

### 6.1. CASE 01

Figure 9 presents the obtained simulation results under a step-speed reference, deliberately avoiding the influence of the ED to evaluate the controller's performance in a basic scenario. This setup allows for a clear analysis of the FASMC's characteristics and effectiveness. As observed in Figure 9(a), the speeds of the IMs on all four wheels are identical, confirming that the ED is inactive in this test. Figure 9(b) illustrates the flux response of the motor under these conditions, further validating the robustness of the proposed control strategy. When Load torques are applied between 2s and 4s, Figure 9(c) shows that the primary variation occurs in the direct torque response, and in the variation of the current in the same interval as seen in Figure 9(d). The developed motor torque is clearly affected, as evidenced by the smooth and logical response in the current waveforms. The presence of a slope contributes to an electromagnetic torque improvement on both the left and right motors.

### 6.2. CASE 02

Figure 10 presents the simulation results following a sudden change in the speed setpoint. These tests, performed in the MATLAB/Simulink environment, are designed to assess the robustness and adaptability of the proposed FASMC strategy in maintaining accurate speed regulation under abrupt disturbances. The results demonstrate the controller's capability to quickly react and stabilize the system, highlighting its effectiveness in handling dynamic variations. Figure 10(a) demonstrates the motor speed response across five speed levels, highlighting precise tracking without overshoot or control errors. Figure 10(b) illustrates the corresponding flux response, while Figure 10(c) displays a smooth torque response, even at low speeds, which is further confirmed by the stable and continuous current profile as illustrated in Figure 10(d).

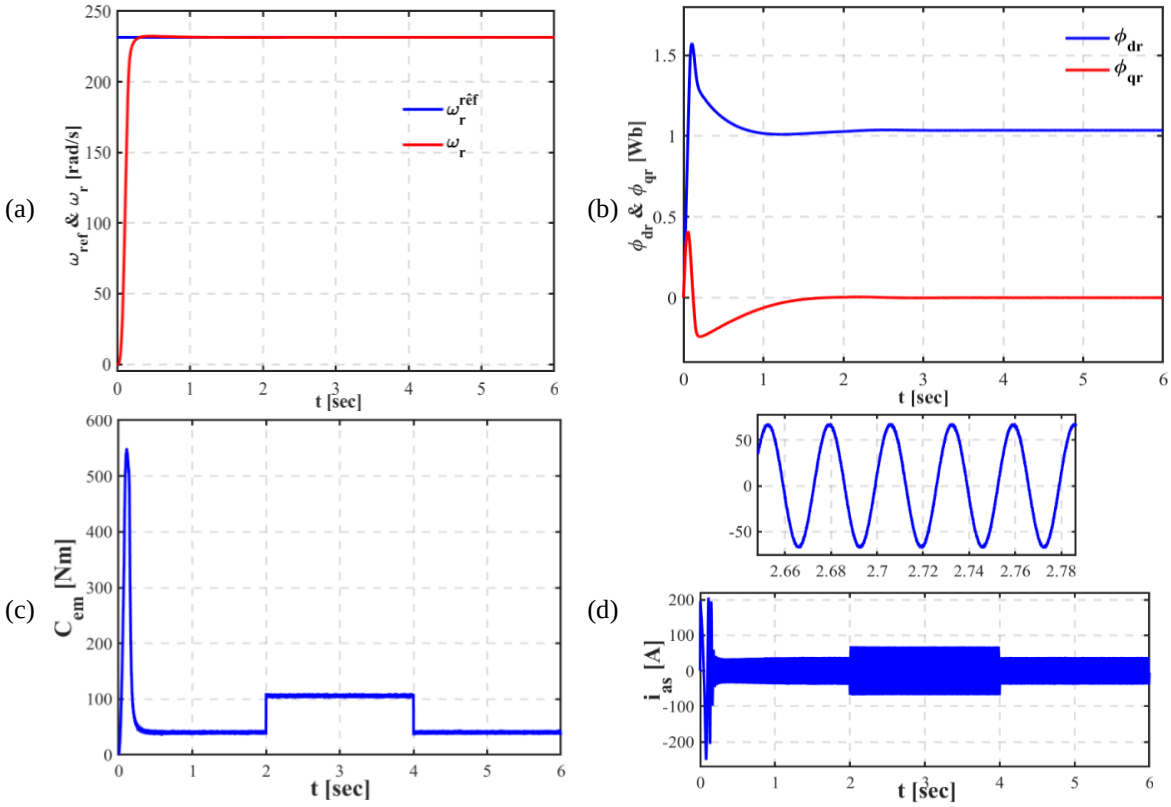


Figure 9. Simulation results: (a) speed responses and its reference [rpm], (b) flux [Wb], (c) electromagnetic torque [N.m], and (d) stator current (A)

Table 4. Nominal system parameter values

| Nominal IM parameter values | | EV mechanical & aerodynamic parameters | |
|---|---|---|---|
| Parameter | Value | Parameter | Value |
| Rated power$P_n$ | 37 Kw | $m$ | 150 kg |
| Line-Line voltage $V_n$ | 400 V | $A$ | 1.8 m$^2$ |
| Rated current $I_n$ | 64 A | $R$ | 0.3 m |
| Rated speed $\omega_n$ | 2960 rpm | $\mu_{rr1}$ | 0.0055 |
| Number of pole pairs $P$ | 1 | $\mu_{rr2}$ | 0.056 |
| Stator resistance $R_s$ | 85.1 mΩ | $Cad$ | 0.19 |
| Rotor resistance $R_r$ | 65.8 mΩ | G | 104 |
| Stator inductance $L_s$ | 31.4 Mh | $\eta_g$ | 0.95 |
| Rotor inductance $L_r$ | 31.4 mH | T | 57.2 Nm |
| Magnetizing inductance $L_m$ | 29.1 mH | $v_0$ | 4.155 m/s |
| Inertia moment of motor $j$ | 0.23 kg/m$^2$ | $g$ | 9.81 m/s$^2$ |
| Friction coefficient $f_c$ | 0.0095 Nm.s/rad | $\rho$ | 0.23 kg/m$^3$ |

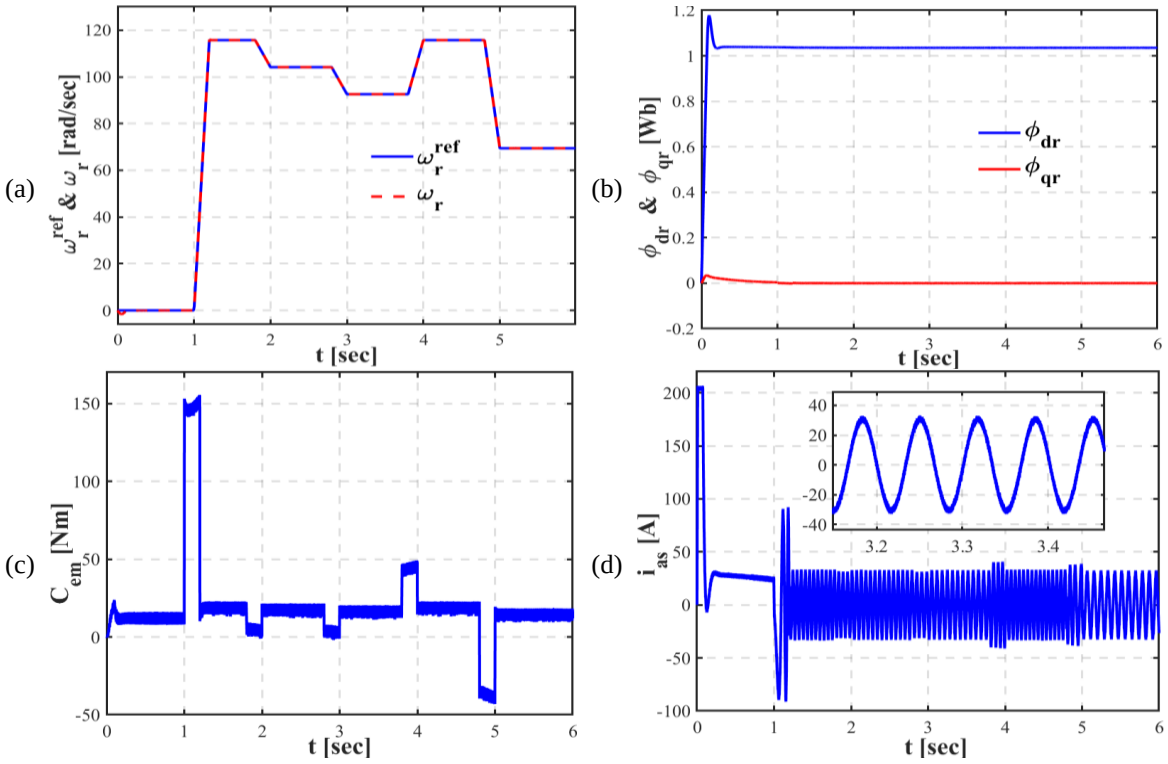


Figure 10. FASMC Simulation results: (a) speed responses and its reference [rpm], (b) flux [Wb], (c) electromagnetic torque [N.m], and (d) stator current (A)

### 6.3. CASE 03

To validate the FASMC control strategy applied to the 4WD electric vehicle traction system, the system was tested under reference speed variations while simulating realistic driving maneuvers, as illustrated in Figure 11. During this test scenario, the driver commands two distinct steering actions. The first maneuver (Phase 01), corresponding to a left turn, occurs at t = 8 s, followed by a right turn at t = 28 s.

Figures 11(a) and 11(b) present the linear velocity of each wheel and its zoomed view, respectively, during the turning sequences at a constant electric vehicle speed of 100 km/h. These figures clearly demonstrate the speed differentiation among the four wheels during cornering, confirming the precise and real-time intervention of the proposed FASMC-based electronic differential system (EDS). The driver-defined steering angle δ is initially applied to the front wheels.

In response, the EDS dynamically adjusts the individual speeds of all four induction motors. During the right-turn maneuver, the EDS reduces the speed of the inner wheels (right side) while increasing that of the outer wheels (left side), thereby ensuring optimal torque distribution and enhanced turning stability. Specifically, during Phase 01, the front-left and rear-left wheels rotate faster than their right-side counterparts, highlighting the adaptive behavior of the control strategy. The smooth and dynamic response of the wheel speeds is illustrated in Figure 11(c).

Figure 11(d) shows the global load torque applied to the electric vehicle, which varies between 40 Nm and 110 Nm during the test scenario. Figure 11(e) depicts the steering angle profile, where a negative steering angle (δ = −8°) indicates a left turn and a positive angle (δ = 8°) corresponds to a right turn. Finally, Figure 11(f) illustrates the electric vehicle speed regulation at 100 km/h, exhibiting no visible overshoot and a maximum deviation of approximately 0.4%.

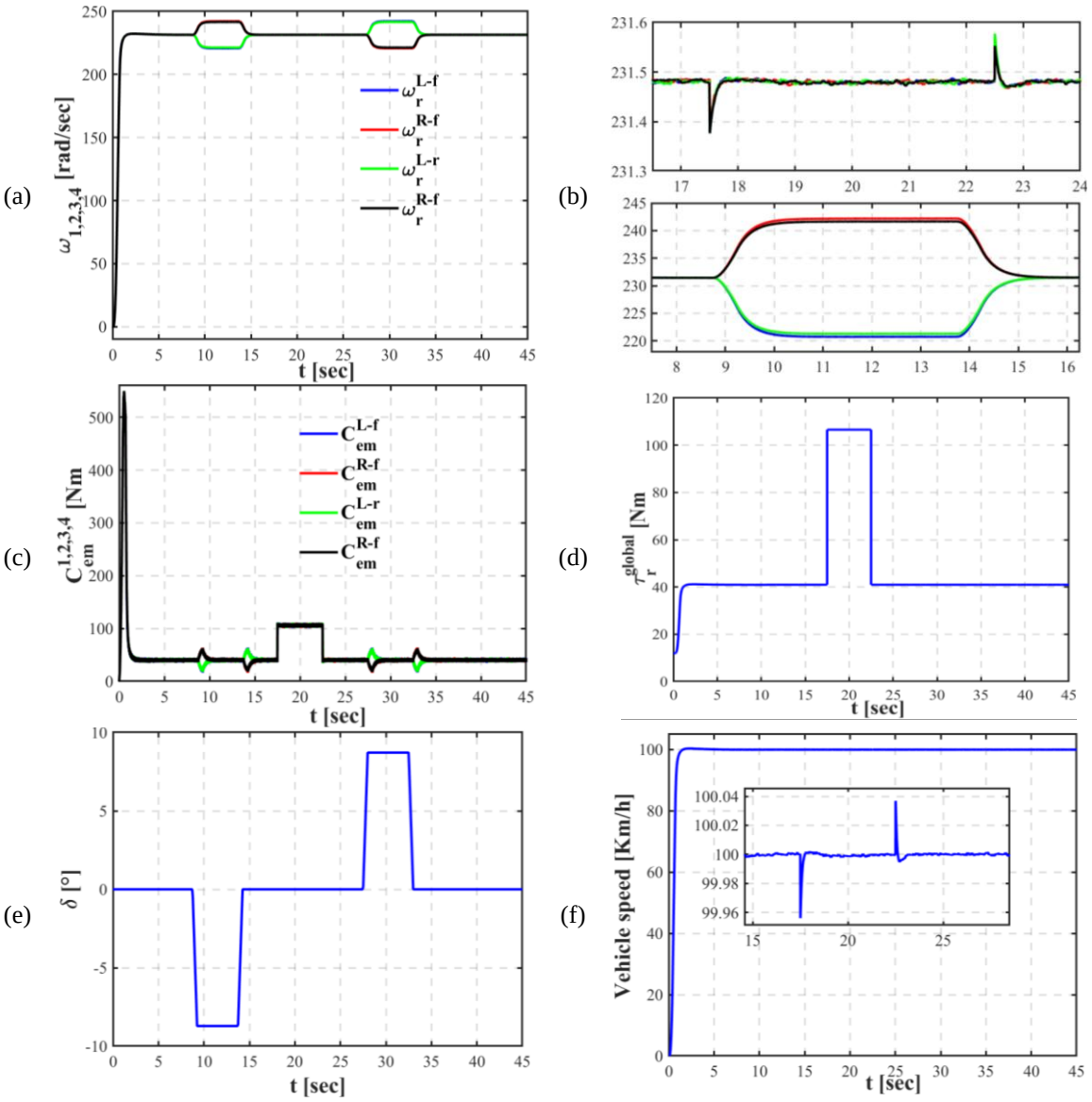


Figure 11. Simulation results of EV behavior: (a) EV wheels speed [rpm], (b) ZOOM of speed, (c) wheels' electromagnetic torque [N.m], (d) load torque (Nm), (e) angle of detour, and (f) EV speed

### 6.4. CASE 04

In this study, the dynamic response of the EV propulsion system is implemented and evaluated under the standardized New European Driving Cycle (NEDC), which includes both urban (ECE-15) and extra-urban (EUDC) driving phases, offering a comprehensive scenario for assessing energy consumption, motor performance, and system efficiency. During the simulation, the focus is placed on analyzing the current drawn by the electric motor from the power supply across all operational modes of the cycle. These include acceleration phases, where high torque demands significantly increase current consumption; cruising phases, where maintaining steady-state efficiency and minimizing current fluctuations are essential; and deceleration or regenerative braking phases, where the energy recovery potential is critically assessed.

Through detailed examination of the current profiles, key insights are obtained regarding motor efficiency, power electronic losses, and total energy consumption. This analysis further identifies opportunities to optimize control strategies, such as FOC or MPC, to reduce energy losses and extend battery life. In addition, the simulated current waveforms are compared with ideal theoretical models to detect deviations caused by nonlinear motor characteristics, switching harmonics, and load variations. These results provide a deeper understanding of real-world energy usage and validate the proposed FASMC strategy's effectiveness in minimizing peak current demand while maintaining robust driving performance throughout the NEDC. Figure 12 illustrates the EV scenario over a duration of 1200 seconds, where Figure 12(a) shows the EV speed profile, Figure 12(b) presents the electromagnetic torque for each wheel, and Figure 12(c) depicts the variation of load torque under realistic driving conditions.

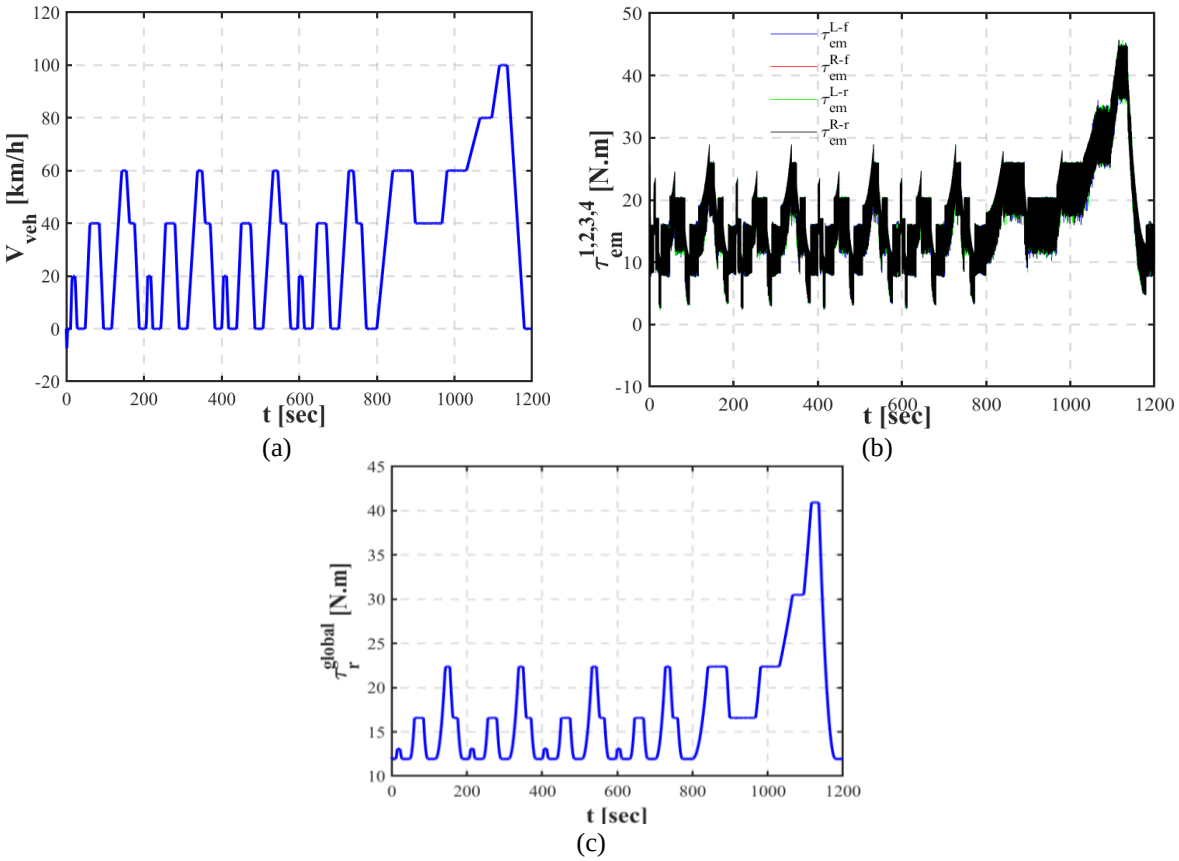


Figure 12. EV scenario: (a) European driving cycle (EDC) speed profile applied to the 4WD electric vehicle [Kw/h], (b) electromagnetic torque response under the proposed control strategy [N.m], and (c) load torque variation corresponding to realistic driving conditions [N.m]

Table 5 presents a comparative analysis between the proposed FASMC-based control strategy and an existing method employing PI and fuzzy logic controllers for 4WDEV speed regulation. As highlighted in the table, the proposed approach outperforms the reference method across several critical aspects. Unlike the conventional FLC and PI strategies, which offer limited robustness and are susceptible to performance degradation under varying conditions, the AFSMC integrates an exponential reaching law with a fuzzy adaptation mechanism to dynamically tune control gains. This significantly reduces chattering and enhances system robustness and tracking accuracy. Moreover, the proposed strategy demonstrates superior adaptability to complex driving scenarios, including slope variation, curved paths, and the NEDC standard cycle, while maintaining better energy efficiency and motor current regulation. Stability is also formally proven using Lyapunov theory, which further confirms the reliability of the proposed method. Overall, the table clearly emphasizes the practical and theoretical advantages of the FASMC approach, making it a promising candidate for advanced EV motion control systems.

Table 5. The comparison of the obtained results with existing published results

| Criterion | This paper | [31] |
|---|---|---|
| Control method | Hybrid SMC with exponential reaching law + fuzzy adaptive gain | Classical PI & FLC |
| Main objective | Reduce chattering, enhance robustness, and tracking performance under dynamic conditions | Compare PI and FLC for speed control in direct torque control (DTC)-based 4WDEV |
| Vehicle architecture | 4WD Electric vehicle with field-oriented control (FOC) and electronic differential system | 4 In-Wheel Induction Motors with DTC |
| Disturbance rejection | High due to fuzzy-tuned adaptive SMC and dynamic gain adjustment | Moderate FLC improves over PI but lacks the robust structure of SMC |
| Chattering reduction | Significantly reduced via the exponential reaching law and fuzzy tuning | Not addressed explicitly, DTC generally suffers from torque ripple |
| Adaptability to road conditions | Excellent includes tests on slope, curves, variable speed, and NEDC cycle | Tested on different road conditions, but control is limited to FLC and PI capabilities |
| Simulation scenarios | Step change, slope resistance, curved path, and standard NEDC driving cycle | Straight, sloped, and curved roads only |
| Implementation complexity | Moderate adaptive fuzzy tuning of SMC enhances control without a high computational load | Lower, simpler PI and FLC, but less robust under uncertainties |
| Stability guarantee | Proven via Lyapunov stability analysis | |

## 7. CONCLUSION

This paper presented a FASMC strategy to enhance speed tracking performance in a 4WD EV. Unlike conventional sliding mode controllers, which are often affected by chattering and limited adaptability, the proposed approach incorporates a fuzzy logic–based mechanism to dynamically adjust the switching gain, thereby improving control accuracy, robustness, and overall system stability.

Simulation results under various driving conditions demonstrated improved dynamic behavior, characterized by reduced chattering, faster torque and flux responses, and enhanced transient performance. The improved control smoothness contributes to better energy utilization, particularly during startup and rapid speed variations.

The developed control framework is suitable for real-time implementation due to its computational efficiency and compatibility with embedded platforms such as microcontrollers and digital signal processors commonly employed in electric vehicle control systems.

Although the method involves relatively complex mathematical formulations, it remains practical for advanced control applications. Future work will focus on optimizing the computational efficiency of the fuzzy inference mechanism for real-time deployment and investigating its integration with additional vehicle subsystems, including regenerative braking and energy management, to establish a comprehensive and coordinated control architecture.

## FUNDING INFORMATION

The authors declare that no funds, grants, or other support were received during the preparation of this manuscript.

## AUTHOR CONTRIBUTIONS STATEMENT

This journal uses the Contributor Roles Taxonomy (CRediT) to recognize individual author contributions, reduce authorship disputes, and facilitate collaboration.

| Name of Author | C | M | So | Va | Fo | I | R | D | O | E | Vi | Su | P | Fu |
|---|---|---|---|---|---|---|---|---|---|---|---|---|---|---|
| Abdelhamid Bouregba | ✓ | ✓ | ✓ | ✓ | ✓ | ✓ | | ✓ | ✓ | ✓ | | | ✓ | |
| Abdeldjabar Hazzab | | ✓ | | | | ✓ | | ✓ | ✓ | ✓ | ✓ | ✓ | | |
| Aissa Benhammou | ✓ | | ✓ | ✓ | | | ✓ | | | ✓ | ✓ | | ✓ | ✓ |
| Samir Hadjeri | | | | | ✓ | | ✓ | | | ✓ | | ✓ | | ✓ |

C : **C**onceptualization
M : **M**ethodology
So : **So**ftware
Va : **Va**lidation
Fo : **Fo**rmal analysis
I : **I**nvestigation
R : **R**esources
D : **D**ata Curation
O : Writing - **O**riginal Draft
E : Writing - Review & **E**diting
Vi : **Vi**sualization
Su : **Su**pervision
P : **P**roject administration
Fu : **Fu**nding acquisition

## CONFLICT OF INTEREST STATEMENT

The authors declare that they have no conflicts of interest to disclose.

## DATA AVAILABILITY

The data availability is not applicable to this paper as no new data were created or analyzed in this study.

## REFERENCES


[1] A. Kimouche, M. R. Mekideche, M. Chebout, and H. Allag, "Influence of permanent magnet parameters on the performances of claw pole machines used in hybrid vehicles," *Electrical Engineering and Electromechanics*, vol. 2024, no. 4, pp. 3–8, Jun. 2024, doi: 10.20998/2074-272X.2024.4.01.

[2] M. M. Islam *et al.*, "Improving Reliability and Stability of the Power Systems: A comprehensive review on the role of energy storage systems to enhance flexibility," *IEEE Access*, vol. 12, pp. 152738–152765, 2024, doi: 10.1109/ACCESS.2024.3476959.

[3] B. Aissa, T. Hamza, G. Yacine, and H. M. Amine, "Impact of artificial intelligence in renewable energy management of hybrid systems," *Physical Sciences Forum*, vol. 6, no. 1, p. 5, 2023, doi: 10.3390/psf2023006005.

[4] L. Djafer *et al.*, "Electric drive vehicle based on sliding mode control technique using a 21-level asymmetrical inverter under different operating conditions," *Electrical Engineering and Electromechanics*, vol. 2025, no. 3, 2025, doi: 10.20998/2074-272X.2025.3.05.

[5] K. Abed and H. K. E. Zine, "Intelligent fuzzy back-stepping observer design based induction motor robust nonlinear sensorless control," *Electrical Engineering and Electromechanics*, vol. 2024, no. 2, pp. 10–15, Feb. 2024, doi: 10.20998/2074-272X.2024.2.02.

[6] O. Oussama, D. Kerdoun, and A. Boumassata, "Comparative study between sliding mode control and the vector control of a brushless doubly fed reluctance generator based on wind energy conversion systems," *Electrical Engineering and Electromechanics*, no. 1, pp. 51–58, Feb. 2022, doi: 10.20998/2074-272X.2022.1.07.

[7] O. Oualah, D. Kerdoun, and A. Boumassata, "Super-twisting sliding mode control for brushless doubly-fed reluctance generator based on wind energy conversion system," *Electrical Engineering and Electromechanics*, vol. 2023, no. 2, pp. 86–92, Mar. 2023, doi: 10.20998/2074-272X.2023.2.13.

[8] D. Sakri, H. Laib, S. E. Farhi, and N. Golea, "Sliding mode approach for control and observation of a three phase AC-DC pulse-width modulation rectifier," *Electrical Engineering and Electromechanics*, vol. 2023, no. 2, pp. 49–56, Mar. 2023, doi: 10.20998/2074-272X.2023.2.08.

[9] D. Cherifi and Y. Miloud, "Hybrid control using adaptive fuzzy sliding mode control of doubly fed induction generator for wind energy conversion system," *Periodica Polytechnica Electrical Engineering and Computer Science*, vol. 64, no. 4, pp. 374–381, Sep. 2020, doi: 10.3311/PPee.15508.

[10] F. F. M. El-Sousy, M. M. Amin, and O. A. Mohammed, "Robust adaptive neural network tracking control with optimized super-twisting sliding-mode technique for induction motor drive system," *IEEE Transactions on Industry Applications*, vol. 58, no. 3, pp. 4134–4157, May 2022, doi: 10.1109/TIA.2022.3160136.

[11] D. Cherifi and Y. Miloud, "Hybrid control using adaptive fuzzy sliding mode control of doubly fed induction generator for wind energy conversion system," *Periodica Polytechnica Electrical Engineering and Computer Science*, vol. 64, no. 4, pp. 374–381, 2020, doi: 10.3311/PPee.15508.

[12] A. Benhammou, M. A. Hartani, H. Tedjini, H. Rezk, and M. Al-Dhaifallah, "Improvement of autonomy, efficiency, and stress of fuel cell hybrid electric vehicle system using robust controller," *Sustainability (Switzerland)*, vol. 15, no. 7, 2023, doi: 10.3390/su15075657.

[13] J. Guo, K. Li, J. Fan, Y. Luo, and J. Wang, "Neural-fuzzy-based adaptive sliding mode automatic steering control of vision-based unmanned electric vehicles," *Chinese Journal of Mechanical Engineering (English Edition)*, vol. 34, no. 1, p. 88, Sep. 2021, doi: 10.1186/s10033-021-00597-w.

[14] G. Q. Geng, P. Cheng, L. Q. Sun, X. Xu, and F. Shen, "A study on lateral stability control of distributed drive electric vehicle based on fuzzy adaptive sliding mode control," *International Journal of Automotive Technology*, vol. 25, no. 6, pp. 1415–1429, 2024, doi: 10.1007/s12239-024-00099-3.

[15] M. Baba, F. Bounaama, S. Bennaceur, A. Benhammou, and M. A. Soumeur, "A particle swarm optimization based fuzzy FLCPi-PSO controller for quadcopter system," *Communications - Scientific Letters of the University of Žilina*, vol. 26, no. 3, pp. C9–C20, 2024, doi: 10.26552/com.C.2024.027.

[16] T. Huang, X. Gao, and T. Li, "Adaptive fuzzy attitude sliding mode control for a quadrotor unmanned aerial vehicle," *International Journal of Fuzzy Systems*, vol. 26, no. 2, pp. 686–701, Mar. 2024, doi: 10.1007/s40815-023-01628-5.

[17] Q. Shi, M. Wang, Z. He, C. Yao, Y. Wei, and L. He, "A fuzzy-based sliding mode control approach for acceleration slip regulation of battery electric vehicle," *Chinese Journal of Mechanical Engineering (English Edition)*, vol. 35, no. 1, p. 72, Jun. 2022, doi: 10.1186/s10033-022-00729-w.

[18] T. A. Nguyen, "A novel approach with a fuzzy sliding mode proportional integral control algorithm tuned by fuzzy method (FSMPIF)," *Scientific Reports*, vol. 13, no. 1, p. 7327, May 2023, doi: 10.1038/s41598-023-34455-7.

[19] G. Torrente, E. Kaufmann, P. Fohn, and D. Scaramuzza, "Data-driven MPC for quadrotors," *IEEE Robotics and Automation Letters*, vol. 6, no. 2, pp. 3769–3776, 2021, doi: 10.1109/LRA.2021.3061307.

[20] A. Benhammou, M. A. Hartani, and I. E. Kimi, "Metaheuristic optimization of fractional-order PID controllers for quadcopter system," in *Proceedings of EDiS 2024 - 2024 4th International Conference on Embedded and Distributed Systems*, IEEE, 2024, pp. 314–319. doi: 10.1109/EDiS63605.2024.10783289.

[21] F. Ziani, A. Benhammou, M. A. Hartani, and H. Rezk, "Quadrotor robust fractional-order control based on a recent bonobo optimization algorithm," *Journal of Mathematics*, vol. 2025, no. 1, p. 2065604, 2025, doi: 10.1155/jom/2065604.

[22] A. Haddoun, M. E. H. Benbouzid, D. Diallo, R. Abdessemed, J. Ghouili, and K. Srairi, "Modeling, analysis, and neural network control of an ev electrical differential," *IEEE Transactions on Industrial Electronics*, vol. 55, no. 6, pp. 2286–2294, 2008, doi: 10.1109/TIE.2008.918392.

[23] L. Baghli, "Contribution to induction machine control: using fuzzy logic, neural networks and genetic algorithms," Doctoral Thesis, Henri Poincare University, 1999.

[24] V. I. Utkin, "Sliding mode control design principles and applications to electric drives," *IEEE Transactions on Industrial Electronics*, vol. 40, no. 1, pp. 23–36, 1993, doi: 10.1109/41.184818.

[25] Q. Shi, M. Wang, Z. He, C. Yao, Y. Wei, and L. He, "A fuzzy-based sliding mode control approach for acceleration slip regulation of battery electric vehicle," *Chinese Journal of Mechanical Engineering (English Edition)*, vol. 35, no. 1, 2022, doi: 10.1186/s10033-022-00729-w.
[26] M. Amine Hartani, A. Benhammou, and A. Laidi, "Performance evaluation of pi and ST-SMC controllers in low voltage/power DC-microgrids," *Advances in Robust Control and Applications*, 2025, doi: 10.5772/intechopen.1006834.
[27] R. J. Wai, "Adaptive sliding-mode control for induction servomotor drive," *IEE Proceedings: Electric Power Applications*, vol. 147, no. 6, pp. 553–562, 2000, doi: 10.1049/ip-epa:20000628.
[28] K. Makhloufi, I. K. Bousserhane, and S. A. Zegnoun, "Adaptive fuzzy sliding mode controller design for PMLSM position control," *International Journal of Power Electronics and Drive Systems (IJPEDS)*, vol. 12, no. 2, pp. 674–684, 2021, doi: 10.11591/ijpeds.v12.i2.pp674-684.
[29] A. Ghezouani, B. Gasbaoui, N. Nair, O. Abdelkhalek, and J. Ghouili, "Comparative study of pi and fuzzy logic based speed controllers of an ev with four in-wheel induction motors drive," *Journal of Automation, Mobile Robotics and Intelligent Systems*, vol. 12, no. 3, pp. 43–54, 2018, doi: 10.14313/JAMRIS_3-2018/17.
[30] A. Nurettin and N. İnanç, "Design of a robust hybrid fuzzy super-twisting speed controller for induction motor vector control systems," *Neural Computing and Applications*, vol. 34, no. 22, pp. 19863–19876, 2022, doi: 10.1007/s00521-022-07519-4.
[31] Q. Nguyen-Vinh and T. Pham-Tran-Bich, "Sliding mode control of induction motor with fuzzy logic observer," *Electrical Engineering*, vol. 105, no. 5, pp. 2769–2780, 2023, doi: 10.1007/s00202-023-01842-2.

## BIOGRAPHIES OF AUTHORS

**Abdelhamid Bouregba** (born 1971, Adrar, Algeria) holds an Engineering Diploma in Electric Power Systems (1999) and a magister degree in automatic control (2013), both from the University of Bechar. He is currently a Ph.D. candidate in electrical engineering at Djillali Liabes University, Sidi-bel-Abbès. His research focuses on electric drives, electric vehicles, and modern control methods. He can be contacted at email: hamidgourarii@gmail.com.

**Abdeldjebar Hazzab** received the State Engineer degree in Electrical Engineering from the University of Sciences and Technology of Oran (USTO), Algeria, in 1995. He continued his studies at USTO, earning an M.Sc. degree in 1999 and a Ph.D. degree in 2006, both from the Electrical Engineering Institute. He is currently a professor of Electrical Engineering at the University of Bechar, Algeria, where he serves as the Director of the Research Laboratory for the Analysis, Control, and Optimization of Electrified Energetic Systems. Additionally, he is an Invited Professor at the École de Technologies Supérieure (ETS), Université du Québec, Montréal, Canada. His research interests include power electronics, control of electric drives, and artificial intelligence, along with their applications. He can be contacted at email: hazzab.abdeldjebar@etsmtl.ca or abdeldjebar.hazzab@gmail.com.

**Aissa Benhammou** holds a Ph.D. in industrial electrotechnics. He earned his master's degree from Tahri Mohamed University of Becher, and completed his Ph.D. at the Nour Elbachir University Center of El-Bayadh. His research interests encompass electric vehicles, drone systems, power electronics, optimization algorithms, and electrostatic separation. He can be contacted at email: benhammou.aissa@univ-bechar.dz.

**Samir Hadjeri** holds an Electrical Engineering diploma from the University of Science and Technology of Oran, Algeria, a master's degree from Laval University, Canada (1990), and a Ph.D. from the University of Djillali Liabes, Algeria (2003). A longstanding member of the academic community, he is now a professor and Dean of the Faculty at Djillali Liabes University. He can be contacted email: shadjeri2@yahoo.fr.